

## Current status of Venus orbiter Akatsuki

NAKAMURA, Masato<sup>1\*</sup>, IMAMURA, Takeshi<sup>1</sup>

<sup>1</sup>Institute of Space and Astronautical Science, Japan Aerospace Exploration Agency

The first Venus probe of Japan, Akatsuki, was launched in May 2010. The Venus orbit insertion maneuver conducted in December 2010 has failed due to a malfunction of the propulsion system, and at present the spacecraft is orbiting the Sun. Akatsuki will have a chance to encounter Venus in 2015; the project team is examining the possibility of conducting an orbit insertion maneuver again at this opportunity.

Keywords: Venus, exploration, Akatsuki

## Atmospheric structure in the cloud-top altitude region of Venus

TAGUCHI, Makoto<sup>1\*</sup>, FUKUHARA, Tetsuya<sup>2</sup>, FUTAGUCHI, Masahiko<sup>1</sup>, IMAMURA, Takeshi<sup>3</sup>, NAKAMURA, Masato<sup>3</sup>, UENO, Munetaka<sup>3</sup>, IWAGAMI, Naomoto<sup>4</sup>, SATO, Mitsuteru<sup>2</sup>, MITSUYAMA, Kazuaki<sup>4</sup>, HASHIMOTO, George<sup>5</sup>

<sup>1</sup>Rikkyo University, <sup>2</sup>Hokkaido University, <sup>3</sup>ISAS, <sup>4</sup>University of Tokyo, <sup>5</sup>Okayama University

The first Japanese Venus orbiter Akatsuki launched in May 2010 is a meteorological satellite which will reveal the 3-D structure of Venusian atmosphere using 5 cameras and a radio occultation experiment onboard. The Longwave Infrared Camera is one of the suite of cameras and measures thermal infrared radiation in the wavelength region of 8-12  $\mu\text{m}$  emitted from the cloud-top altitude region around 65 km. Observed data is converted to brightness temperature with absolute temperature accuracy of 3 K and noise-equivalent temperature difference of 0.3 K using an algorithm developed by the pre-launch calibration experiment. Akatsuki arrived at Venus on December 7, 2010, but unfortunately the Venus orbit insertion was failed. While Akatsuki was traveling away from Venus, LIR acquired a few Venus images on December 9 and 10. The downloaded image is blurred because of spacecraft attitude change during the image acquisition. A clear image was obtained by precise correction of line-of-sight shift which is calculated from the brightness center position of Venus disk imaged in each intermediate image (Fig.1a).

The obtained brightness temperature maps show cloud-top temperature ranging from 225 to 240 K, the cold collar and dipole in the northern polar region, the limb darkening effect due to difference in optical depth versus zenith angle of line-of-sight, zonal structures and finer structures therein seen in the middle and low latitudes, and temporal variation of them. The observed limb darkening was reconstructed by a fitting calculation using model profiles of cloud optical depth and temperature. The retrieved optical depth exhibits a steep gradient at the upper cloud-top region and is 2-8 km lower in altitude than the initial profile. The brightness temperature map was corrected for the limb darkening effect thus calculated (Fig.1b), and compared with ultraviolet images obtained by the Venus Monitoring Camera (VMC) onboard Venus Express.

VMC observes solar light scattered by the cloud particles, while LIR observes thermal infrared radiation from the cloud particles. The light emitting altitude region is almost same for the UV and infrared images, though the observed hemisphere and local time are different. It is found that bright zonal belts exist in the latitude region of -45 to -55 both in the UV and mid-infrared images. This implies that the higher temperature belt where LIR can see deeper through the upper cloud with thin optical depth is laid in the latitude region where density of UV absorber is thin. The fact that the zonal structure extends for all local time suggests the cloud particles seen in the mid-infrared or the UV absorber can live longer than a few days. The mid-infrared images obtained by LIR show the brightness temperature distribution on the almost whole Venus nightside for the first time, and the information retrieved from the images gives constraint on the atmospheric dynamics and cloud chemistry in the cloud-top altitude region of Venusian atmosphere.

### References

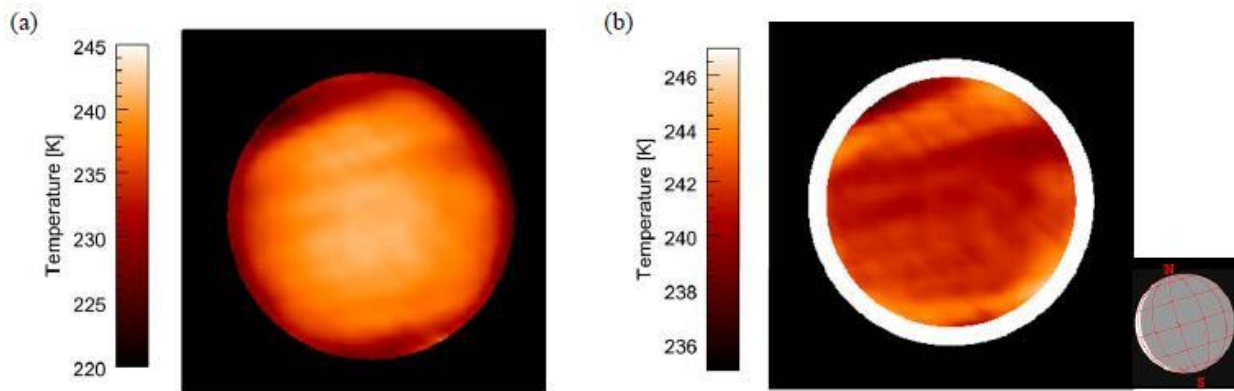
Taguchi et al., *Icarus*, in press, 10.1016/j.icarus.2012.01.024, 2012.

Figure 1. Brightness temperature distributions composited from 32 intermediate images (M=32 and N=32) (a) before and (b) after correction for the limb darkening effect. The illustration in the lower right shows equi-latitude and -longitude lines every 30 degree and the sunlit region of the Venus disk [Taguchi et al., 2012].

PCG33-02

Room:202

Time:May 25 09:15-09:30



**Figure 1**

## Venus' clouds as inferred from the phase curves acquired by IR1 and IR2 on board Akatsuki

SATO, Takehiko<sup>1\*</sup>, OHTSUKI, Shoko<sup>1</sup>, IWAGAMI, Naomoto<sup>2</sup>, UENO, Munetaka<sup>1</sup>, Kazunori Uemizu<sup>1</sup>, SUZUKI, Makoto<sup>1</sup>, HASHIMOTO, George<sup>3</sup>, SAKANOI, Takeshi<sup>4</sup>, KASABA, Yasumasa<sup>4</sup>, NAKAMURA, Ryosuke<sup>5</sup>, IMAMURA, Takeshi<sup>1</sup>, NAKAMURA, Masato<sup>1</sup>, FUKUHARA, Tetsuya<sup>6</sup>, YAMAZAKI, Atsushi<sup>1</sup>, YAMADA, Manabu<sup>1</sup>

<sup>1</sup>Japan Aerospace Exploration Agency, <sup>2</sup>University of Tokyo, <sup>3</sup>Okayama University, <sup>4</sup>Tohoku University, <sup>5</sup>National Institute of Advanced Industrial Science and Technology, <sup>6</sup>Hokkaido University

We present phase curves for Venus in the 1-2 micron wavelength region, acquired with IR1 and IR2 on board Akatsuki (February - March 2011). A large discrepancy with the previously-published curves was found in the small phase angle range ( $0^\circ$  -  $30^\circ$ ). Through analysis by radiative-transfer computation, it was found that the visibility of larger ( $\sim 1$  micron or larger) cloud particles was significantly higher than in the standard cloud model. Although the cause is unknown, this may be related to the recently reported increase in the abundance of  $\text{SO}_2$  in the upper atmosphere. It was also found that the cloud top is located at  $\sim 75$  km and that 1-micron particles exist above the cloud, both of these results being consistent with recent studies based on the Venus Express observations in 2006 - 2008. Further monitoring, including photometry for phase curves, polarimetry for aerosol properties, spectroscopy for  $\text{SO}_2$  abundance, and cloud opacity measurements in the near-infrared windows, is required in order to understand the mechanism of this large-scale change.

Keywords: Venus, phase curve, cloud structure, Akatsuki, IR1, IR2

## Vertical propagation and wind speed acceleration of planetary-scale waves at the cloud level of Venus

KOUYAMA, Toru<sup>1\*</sup>, IMAMURA, Takeshi<sup>2</sup>, NAKAMURA, Masato<sup>2</sup>, SATOH, Takehiko<sup>2</sup>, Futaana Yoshifumi<sup>3</sup>

<sup>1</sup>University of Tokyo, <sup>2</sup>ISAS/JAXA, <sup>3</sup>Swedish Institute of Space Physics

In this study, we reveal temporal variation of the super-rotation of Venus atmosphere and spatial structures of planetary scale atmospheric waves at the cloud top level by deriving wind speeds and their variations at the cloud top from UV (365 nm) images taken by Venus Monitoring Camera (VMC) onboard Venus Express of European Space Agency. Because VMC has taken many cloud images covering from low to high latitudes of the southern hemisphere, well suited for derivation of wind speeds and their variations. We applied a newly-developed cloud tracking method (Ogohara et al., 2012; Kouyama et al., 2012) to these images and found that the equatorial zonal wind speed changes quasi-periodically, alternating "fast season" (over  $100 \text{ m s}^{-1}$ ) and "slow season" (below  $90 \text{ m s}^{-1}$ ) every  $\sim 100$  earth days.

From spectral analysis of the wind speed and the cloud brightness variations, planetary-scale 5 day period variations were identified in the zonal and meridional wind speeds in the fast season of background zonal wind speeds. The phase speed of the 5-day period variations is slower than the background wind speed. The phase relationship between the zonal and meridional winds implies that the 5-day variation is a manifestation of a Rossby wave. On the other hand, planetary-scale 4 day period variations were identified in zonal wind speeds and cloud brightness in the slow season. The phase speed of the 4-day period variations is faster than the background wind speed. These results are consistent with previous studies from Pioneer Venus observations (Del Genio and Rossow, 1990; Rossow et al., 1990).

From the numerical results based on Covey & Schubert (1982), we found that the Kelvin wave originating from the lower atmosphere can propagate vertically into the cloud top level in the slow period. On the other hand, the Rossby wave can propagate in the fast period. Therefore, the time variation of the super-rotation could be affected by these waves. In this study, we will evaluate the angular momentum transport by these waves based on the derived parameters from our analysis.

Keywords: Venus, super-rotation, atmospheric waves

## Investigation of the HDO/H<sub>2</sub>O ratio in the Venus atmosphere from comparison with SOIR on board Venus Express

MATSUI, Hiroki<sup>1\*</sup>, IWAGAMI, Naomoto<sup>1</sup>

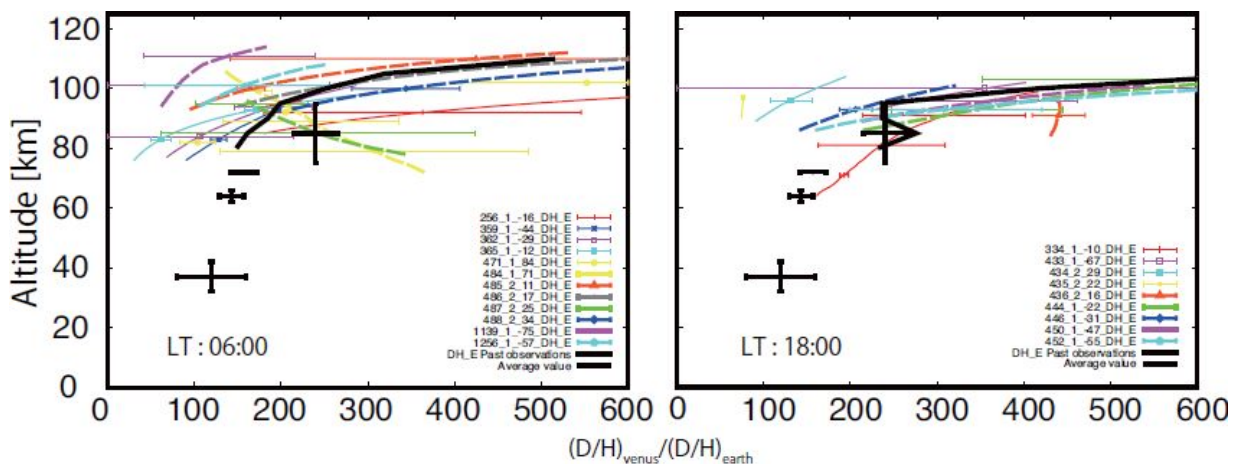
<sup>1</sup>University of Tokyo

By using the IRTF 3 m telescope in Hawaii in 2010, we obtained a disk-averaged HDO mixing ratio of 0.22 +/- 0.03 ppm for a representative height of 62-67 km. Based on previous H<sub>2</sub>O measurements, the HDO/H<sub>2</sub>O ratio there is found to be 140 +/- 20 times larger than the telluric ratio. This lies in between the ratios of 120 +/- 40 and 240 +/- 25, respectively, reported for the 30-40 km region (de Bergh et al. 1991) by ground-based night-side spectroscopy and for the 80-100 km region by solar occultation measurement on board the Venus Express (Fedorova et al. 2008). However, such a large difference between the 62-67 km and 80-100 km regions might be latitudinal not vertical origin because of localization of VEx data mostly at high latitudes. In addition, the measurement by Krasnopolsky (2010) in the evening at an altitude of 70 km shows a latitudinal structure showing an equatorial minimum. This is inconsistent to our measurements.

By examining measurements by SOIR on board Venus Express at the terminator, we tried to check the consistency with our data set, and succeeded to confirm larger D/H ratio at higher altitude with little latitudinal gradient although the D/H ratio seems to be very variable.

Fedorova A. et al. JGR 113 E00B22 2008  
 Krasnopolsky A. Icarus 209 314-322 2010  
 de Bergh et al. Science 251 547-549 1991

Keywords: Venus, HDO, spectroscopy, D/H ratio



## Evidence of ion acceleration by the local convection electric field: Venus Express observations

MASUNAGA, Kei<sup>1\*</sup>, FUTAANA, Yoshifumi<sup>2</sup>, YAMAUCHI Masatoshi<sup>2</sup>, TERADA, Naoki<sup>1</sup>, OKANO, Shoichi<sup>1</sup>

<sup>1</sup>Grad. Sch. of Sci., Tohoku Univ., <sup>2</sup>Swedish Institute of Space Physics

Venus has no intrinsic magnetic field, so its upper atmosphere is directly exposed to the solar wind creating direct interactions between them. As a result of the interaction, ionospheric ions are removed from Venus mainly as O<sup>+</sup>. It is thought that the escaping oxygen from the atmosphere has played an important role in the atmospheric evolution on Venus. Pioneer Venus Orbiter and Venus Express have investigated the plasma environment of Venus. Many authors reported that high energy planetary oxygen ions were observed in the hemisphere to which a global convection electric field ( $E_{sw} = -V_{sw} \times B_{sw}$ ) directs [e.g., Intriligator, 1989, Slavin et al., 1989; Barabash et al., 2007]. Thus, the convection electric field has been considered as a possible mechanism for the acceleration of planetary ions.

However, recently Masunaga et al., [2011] reported that a spatial distribution of outflowing O<sup>+</sup> ions is strongly controlled by the IMF directions. By investigating two cases, IMF directs nearly perpendicular to the Venus-Sun line (perpendicular IMF case) and IMF directs nearly parallel to it (parallel IMF case), they indicated that the O<sup>+</sup> ion acceleration mechanisms would be different. In the perpendicular IMF case, O<sup>+</sup> fluxes are observed near the magnetic poles and x-component of the magnetic field reverses once per orbit. Sometimes the O<sup>+</sup> flux is associated with the B<sub>x</sub> reversal. Energy of those fluxes depends on the global convection electric field, which is consistent with previous studies [e.g. Intriligator, 1989; Slavin et al., 1989; Barabash et al., 2007]. These results can be understood by draping of the IMF around the Venus ionosphere followed by forming a single plasma sheet, and thus most of O<sup>+</sup> ions are accelerated by the convection electric field and outflow through the plasma sheet. On the other hand in the parallel IMF case, a spatial distribution of O<sup>+</sup> is different from that of the perpendicular IMF case. O<sup>+</sup> fluxes are observed regardless of the convection electric field direction and B<sub>x</sub> reverses multiple times per orbit. The fluxes are sometimes associated with the B<sub>x</sub> reversal. Energy of the fluxes does not depend on the direction of the global magnetic field. This indicates that IMF drapes around the ionosphere more complicatedly and forms multiple outflow channels around the terminator. The independency of the outflow channel and the convection electric field direction indicates that O<sup>+</sup> ions are not accelerated by the convection electric field but by local effects, such as a  $j \times B$  force [Dubinin et al., 1993], viscous force [Perez-de-Tejada, 1997] or local convection electric field ( $E_L = -V_L \times B_L$ ; where  $V_L$  and  $B_L$  is the local velocity vector and the local magnetic field).

In this study we concentrate on the effect of the local convection electric field and discuss whether or not the local electric field can explain the O<sup>+</sup> acceleration observed by Venus Express. We show several examples to investigate dependence of oxygen ions' flow direction on the local convection electric field's direction by comparing with the global convection electric field's direction. The dependence between the O<sup>+</sup> velocity vector and the local convection electric field is clearer than that on the global convection electric field in both cases. This may imply that planetary O<sup>+</sup> ions could be accelerated by the local convection electric field.

### References

- Barabash et al., [2007], Nature, 450, 650-653, doi:10.1038/nature06434.
- Dubinin et al., [1993], JGR, 98, A3, 3991-3997
- Intriligator, [1989], GRL, 16, 2, 167-170
- Masunaga et al., [2011], JGR, 116, A09326
- Perez-de-Tejada, JGR, 106, A1, 211-219, 2001
- Slavin et al., [1989], JGR, 94, A3, 2383-2398

Keywords: Venus, ASPERA, outflow, escape



## Effects of the solar wind electric field on heavy-ion precipitation onto the Martian atmosphere: A statistical survey

HARA, Takuya<sup>1\*</sup>, SEKI, Kanako<sup>1</sup>, FUTAANA, Yoshifumi<sup>2</sup>, YAMAUCHI Masatoshi<sup>2</sup>, BARABASH Stas<sup>2</sup>, FEDOROV Andrei<sup>3</sup>

<sup>1</sup>STEL, Nagoya Univ., <sup>2</sup>IRF, Kiruna, Sweden, <sup>3</sup>CESR, Toulouse, France

The solar wind can directly interact with the Martian upper atmosphere, since Mars does not possess a global intrinsic magnetic field [e.g., Acuna *et al.*, 1998]. Atmospheric escape phenomena induced by the solar wind interaction have been observed by Phobos-2 at solar maximum, and recently by Mars Express (MEX) at solar minimum [e.g., Lundin *et al.*, 1989; Barabash *et al.*, 2007]. Escape rates of planetary ions estimated by both spacecraft indicate a large dependence on the solar wind conditions [e.g., Barabash *et al.*, 2007; Lundin *et al.*, 2008]. It has been known that escaping planetary ions, which are picked up by interplanetary magnetic field (IMF) in the solar wind, are distributed highly asymmetrically in terms of the convective electric field [Barabash *et al.*, 2007]. In addition to escaping ions, ions precipitating onto the Martian upper atmosphere should also contribute to atmospheric escape because they collide with atmospheric neutral particles, giving some particles sufficient energy to escape the planet [e.g., Luhmann *et al.*, 1992]. This process is referred as ion sputtering. Ion sputtering could have been a significant escape process for ancient Mars due to the extreme solar EUV radiation, according to some results of numerical simulations [e.g., Luhmann *et al.*, 1992; Leblanc and Johnson, 2002]. However, there are no conclusive in situ measurements of sputtering for Mars.

Precipitating planetary heavy ions with energies of up to a few keV were observed by MEX predominantly during CIR passages [Hara *et al.*, 2011]. Hara *et al.*, [2011] suggested that the flux of precipitating heavy ions is enhanced during CIR events because the gyroradius of picked-up ions is decreased to values comparable to the radius of Mars by the compressed IMF. The direction of the convective electric field in the solar wind should also be important for the behavior of picked-up ions. However, MEX does not carry any magnetic or electric field detectors, and therefore we cannot easily obtain the direction of the magnetic field or that of convective electric field in the solar wind.

Here we attempt to estimate the IMF orientation from MEX ion observations using the ring-like velocity distribution functions of picked-up protons of the exospheric origin [Yamauchi *et al.*, 2006, 2008]. We are able to calculate the IMF orientation from the assumption that the gyration plane of these ions in velocity space is perpendicular to the IMF direction. Then, we conduct simple statistical trajectory tracings of picked up protons in physical space in order to determine the polarity of the IMF. We assume two IMF configurations (differing only in polarity) and traced a number of pickup protons. Then we can determine the polarity of IMF by inspecting which configuration better matches the observation. We also discuss the application of this method to statistically study effects of the solar wind electric field on the heavy-ion precipitation for Mars using the events in which both ring-ions and precipitating heavy ions are observed by MEX in the same orbit.

### References:

- Acuna, M. H., et al. (1998), *Science*, 279, 1676–1680.
- Barabash, S., et al. (2007), *Science*, 315, 501–503.
- Hara, T., et al. (2011), *J. Geophys. Res.*, 116, A02309, doi:10.1029/2010JA015778.
- Leblanc, F. and R. E. Johnson (2002), *J. Geophys. Res.*, 107(E2), 5010.
- Luhmann, J. G., et al. (1992), *Geophys. Res. Lett.*, 19(21), 2151–2154.
- Lundin, R., et al. (1989), *Nature*, 341, 609–612.
- Lundin, R., et al. (2008), *Geophys. Res. Lett.*, 35, L18203.
- Yamauchi, M., et al. (2006), *Space Sci. Rev.*, 126, 239–266.
- Yamauchi, M., et al. (2008), *Planet. Space Sci.*, 56, 1145–1154.

Keywords: Mars, Solar wind interaction, Atmospheric escape, Nonmagnetized planet



## Three dimensional Mars' exosphere : multi-species thermal and nonthermal models

YAGI, Manabu<sup>1\*</sup>, Francois Leblanc<sup>2</sup>, Jean-Yves Chaufray<sup>2</sup>, Ronan Modolo<sup>2</sup>, Sebastien Hess<sup>2</sup>, Francisco Gonzalez-Galindo<sup>3</sup>

<sup>1</sup>STEL, Nagoya University, <sup>2</sup>LATMOS/IPSL, CNRS, France, <sup>3</sup>IAA-CSIC, Granada, Spain

The escaping rate of Mars' atmosphere is an important issue for its evolution. However, to know the atmospheric escape, it is crucial to well describe Mars' upper atmosphere and exosphere. In this presentation, a three dimensional exospheric model of the main constituents of Mars' thermosphere will be presented. This model describes the Martian exosphere as composed of thermal and non-thermal components. The thermal components of the O and CO<sub>2</sub> exospheres are computed from a modified Chamberlain approach which is extended to three dimension including planetary rotation. A Monte Carlo test particle scheme is used to simulate the nonthermal O exosphere produced by dissociative recombination (DR) of O<sub>2</sub><sup>+</sup> in the thermosphere. The thermospheric and ionospheric conditions are calculated by Mars Global Circulation Model (Gonzalez-Galindo et al., Journal of Geophysical Research, 114, 2009). In this presentation, we will present the main results of this work (Yagi et al., Icarus, Submitted, 2012), that is, the seasonal variations of Mars' exosphere and of the atmospheric escape. This work is part of a project named HELIOSARES aiming to describe Mars' interaction with the solar wind by coupling different numerical models.

Keywords: Mars, Exosphere, Atmospheric Escaping, Simulation

## Long-term variability of Na density in Mercury's atmosphere

DAIROKU, Hayato<sup>1\*</sup>, KAMEDA, Shingo<sup>1</sup>, FUSEGAWA, Ayaka<sup>1</sup>, KAGITANI, Masato<sup>2</sup>, OKANO, Shoichi<sup>2</sup>

<sup>1</sup>Rikkyo University, <sup>2</sup>Tohoku University

Mercury has a very thin atmosphere. Its density is only a trillionth that of Earth's atmosphere; therefore, atoms and molecules in Mercury's atmosphere rarely collide. Hence, its atmosphere is called surface bounded exosphere. Atmospheric particles last only for short duration of a few hours in Mercury's atmosphere, indicating that sources of each of the constituents must exist on the planet. Mariner 10 detected H, He, and O, in Mercury's atmosphere; further, Na, K, and Ca were detected by ground-based observations. Atoms of these, Na has ever been made ground-based observations. The three dominant source processes of Na atoms in Mercury's atmosphere are as follows.

- 1.Solar photon hitting the dayside surface of Mercury, Na atoms contained in the material surface are stimulated and emission.
- 2.Solar wind and ions in the magnetosphere hitting the surface of Mercury, and Na atoms get sputtered from the material surface.
- 3.Na atom emission for vaporization when the interplanetary dust on the ecliptic plane hit the surface of Mercury.

However, the most dominant among the abovementioned processes is yet to be clarified. Because of Mercury's proximity to the sun, observations cannot be made from about 30 min before sunrise or after sunset. This makes it impossible to study long-term (more than 1 h) variability of atmospheric density in order to determine the source of Na atoms. We conducted continuous spectroscopic observations of Mercury's exosphere with a 40-cm telescope at Haleakala Observatory in Maui. And we succeeded observation for 10 h during the daytime by replace the hood on the telescope to prevent stray light from hitting the primary mirror directly.

We compared the long-term variability of Na density in Mercury's atmosphere with date on the amount of solar wind particles such as ions and electrons around the planet; this data was obtained from NASA's MESSENGER spacecraft. We suggested a correlative relationship between the solar wind particles and the source processes of Na atoms in Mercury's atmosphere.

Keywords: Mercury, Na, airglow, Ground-based observation, Planetary Atmosphere, MESSENGER

## MHD simulation of Kronian magnetosphere with the high resolution solar wind data

FUKAZAWA, Keiichiro<sup>1\*</sup>, Raymond J. Walker<sup>2</sup>, Stefan Eriksson<sup>3</sup>

<sup>1</sup>Research Institute for Information Technology, Kyushu University, <sup>2</sup>IGPP/UCLA, <sup>3</sup>Laboratory for Atmospheric and Space Physics University of Colorado

In a series of studies we have reported that vortices formed at Saturn's dawn magnetopause in simulations when IMF was northward. We interpreted these vortices as resulting from the Kelvin Helmholtz (K-H) instability. Recently thanks to the developments of in computer performance and numerical calculation techniques, we have been able to perform the global magnetospheric simulations of the magnetosphere with much higher resolution than was previously possible. In these simulations we had sufficient resolution to model the signature of the field-aligned currents from the K-H vortices in Saturn's auroral ionosphere and found small patchy regions of upward field-aligned current which may be related to auroral emissions. Recently, patchy aurorae resembling our results have been reported from Cassini observations.

As a follow on study we have used Cassini observations of the solar wind upstream of Saturn to drive a simulation. Using these solar wind data we simulated the Kronian magnetosphere from 2008-02-12/14:00:31 to 2008-02-13/01:59:31. This simulation required about 1500 hours from 768 processor cores on a 10 TFlops supercomputer system with 1TB memory. Thus in this paper we will show the initial simulation results from the solar wind driven simulation and the configurations of vortices and aurorae at Saturn.

## Scattering Properties of Jovian Aerosols from the Cassini ISS Limb-Darkening Observations

SATO, Takao M.<sup>1\*</sup>, SATOH, Takehiko<sup>2</sup>, KASABA, Yasumasa<sup>1</sup>

<sup>1</sup>Department of Geophysics, Graduate School of Science, Tohoku University, <sup>2</sup>Institute of Space and Astronautical Science, Japan Aerospace Exploration Agency

This study provides new observational constraints on the scattering properties of aerosols in the Jovian upper troposphere and stratosphere. To achieve this objectives, we have analyzed imaging data during the Cassini flyby of Jupiter (October 2000-March 2001, solar phase angle coverage: 0-140 degrees) by utilizing its onboard Imaging Science Subsystem (ISS).

In this study, we present the analysis results of four sets of limb-darkening curves extracted along a bright zone (STrZ) and a dark belt (SEBn) from Jovian images in CB2 (750 nm) and BL1 (455 nm). To explain the solar phase angle behaviors of limb-darkening curves for each data set, we perform the radiative transfer calculations with a simple cloud model and the Mie theory applied to scattering of aerosols.

From these calculations, we find two important characteristics of cloud particles. One is the effective radius of cloud ( $r_{eff,cloud}$ ). The best-fit  $r_{eff,cloud}$  is obtained at 0.3 micron in CB2 and 0.2 micron in BL1. These values are in good agreement with those inferred from previous studies for the diffuse and ubiquitous layer of small particles in the upper troposphere as described in the synthesis works by West et al. (1986, 2004). The other is the real part of the refractive index of cloud ( $n_{r,cloud}$ ). The best-fit  $n_{r,cloud}$  for all data sets except for one data set ( $n_{r,cloud} = 1.8$ ) get a same value ( $n_{r,cloud} = 1.85$ ). Such values of  $n_{r,cloud}$  are found to be much higher than previous experimental values of  $n_r$  for  $NH_3$  ice particles ( $n_r \sim 1.4$ ). Thus, we conclude that the best-fit combination of  $n_{r,cloud}$  and  $r_{eff,cloud}$  would strongly suggest the idea that the abundant small particle population in the upper troposphere is not composed of pure  $NH_3$  ice. What actually eliminates the spectral signature of  $NH_3$  ice around the 3-micron wavelength, despite the fact that significant depletion of  $NH_3$  vapor has been observed for pressure levels of visible cloud layer, is unclear at this moment. The high real refractive index obtained in this study may hint at the composition of cloud particles for further studies.

As described above, the scattering properties of cloud particles for both the STrZ and the SEBn are found to show much the same characteristics, which suggests that the cloud particles themselves are less likely to be related to the visual difference between the zones and belts. We find that only the single scattering albedo of cloud shows a remarkable difference between two regions (this parameter gets a higher value for the STrZ than one for the SEBn), and is one key parameter which causes the visual difference. Our results support the idea proposed by West et al. (1986). Such difference in absorption would be likely to be due to chromophores (unknown coloring agents).

On the basis of these results, we compare our best-fit Mie phase functions for clouds obtained from all data sets with the phase functions derived by Tomasko et al. (1978) from the Pioneer 10 observations. The overall shapes of our Mie phase functions are found to be much flatter than those of their functions. Our Mie phase functions can reproduce the Pioneer 10 observations well. In contrast, Tomasko et al.'s function does not reproduce the Cassini observations. This is attributed to the fact that their phase function is under-constrained, primarily due to a considerable gap in observations for an intermediate solar phase angle (34-109 degrees).

A set of our new Mie phase functions has two advantages over Tomasko et al.'s functions:

1. since the Cassini data do not have a large gap in solar phase angle, the new Mie phase functions are better constrained;
2. the Mie phase function can easily be applied to different wavelengths.

With such characteristics, we now have a set of reliable baseline phase functions that can be used to interpret the ever-changing appearance of Jovian clouds as changes of the vertical cloud structure and/or distribution of chromophores in the atmosphere.

Keywords: Jupiter, atmosphere, aerosol, Cassini, radiative transfer

## Ground-based telescope observation of Jupiter's polar haze

OZAKI, Akihito<sup>1\*</sup>, TAKAHASHI, Yukihiro<sup>1</sup>, Makoto watanabe<sup>1</sup>, WATANABE, Shigeto<sup>1</sup>, FUKUHARA, Tetsuya<sup>1</sup>, SATO, Mitsuteru<sup>1</sup>

<sup>1</sup>Department of CosmoSciences, Graduate School of Science, Hokkaido University

It is known that Jupiter's polar areas have haze which consists of aerosol particles and gas over which the sun-light is scattered. Haze is located in the layer higher than the cloud top so that the scattered light at the deep methane absorption line of 889 nm is much brighter than non-haze area. Horizontal haze structure is seldom investigated.

In this study, imaging observation of Jupiter's polar haze used ground-based 1.6 m reflector named Pirka telescope operated by Hokkaido University. In order to investigate the temporal variation of the structure of the polar haze, image slices of the Jupiter at 889 nm at latitude of 67 degree, the low latitude edge of the polar haze region, are made for the data obtained in the period of 14:00 - 19:00 UT on 29 October 2011 and 10:30 - 15:00 UT on 31 October 2011. It is found that the polar haze has undulating pattern at the low latitude edge of polar haze like as Cassini observation in 2000, but the specific structures are different.

Keywords: Jupiter

## Effect of the solar UV/EUV heating on the intensity and spatial distribution of Jupiter's synchrotron radiation

KITA, Hajime<sup>1\*</sup>, MISAWA, Hiroaki<sup>1</sup>, TSUCHIYA, Fuminori<sup>1</sup>, TAO, Chihiro<sup>2</sup>, MORIOKA, Akira<sup>1</sup>

<sup>1</sup>Planetary Plasma and Atmospheric Research Center, Tohoku University, <sup>2</sup>ISAS/JAXA

Jupiter's synchrotron radiation (JSR) is the emission from relativistic electrons in the strong magnetic field of the inner magnetosphere, and it is the most effective probe for remote sensing of Jupiter's radiation belt from the Earth. Recent intensive observations for JSR reveal short term variations of JSR with the time scale of days to weeks. Brice and McDonough (1973) proposed a scenario for the short term variations (hereafter the B-M scenario); i.e, the solar UV/EUV heating for Jupiter's upper atmosphere drives neutral wind perturbations and then the induced dynamo electric field leads to enhancement of radial diffusion. If such a process occurs at Jupiter, brightness distribution of JSR is also expected to change. That is, it is expected that the dynamo electric field induced by diurnal neutral wind system produces dawn-dusk electric potential difference and dawn-dusk asymmetry in electron spatial distribution. Then, this makes dawn-dusk asymmetry of the JSR brightness distribution.

Preceding studies confirmed the existence of the short term variations in total flux density and its variation corresponds to the solar UV/EUV variations (Tsuchiya et al., 2011). However, the effect of solar UV/EUV heating on the brightness distribution of JSR has not been confirmed. Hence, the purpose of this study is to confirm the solar UV/EUV heating effect on total flux density and brightness distribution simultaneously, so as to evaluate the B-M scenario. In order to accomplish this purpose, we have made radio imaging analysis using the National Radio Astronomy Observatory (NRAO) archived data with the Very Large Array (VLA) obtained for about 10 days from January to February, 2000. We derived the total flux density and the dawn-dusk peak emission ratio of JSR and examined their relationship to the variation of the solar UV/EUV flux. From the VLA data analysis, following results were shown.

- 1, Total flux density variations occurred corresponding to the solar UV/EUV variations.
- 2, The dawn side emission was brighter than dusk side emission almost every day.
- 3, Variations of the dawn-dusk asymmetry did not correspond to the solar UV/EUV variations.

When we see a dawn-dusk ratio at the long term view (a week order), the second result supports the B-M scenario. However, from the third result, the observed variation feature of the dawn-dusk ratio cannot be examined solely by the solar UV/EUV heating. There is a possibility that variations related to the solar UV/EUV were masked by some other processes which dominated in the variations of the dawn-dusk ratio on the short time scale (day-order).

In order to explain the general features of the dawn-dusk ratio (the second result), we estimate the diurnal wind velocity from the observed dawn-dusk ratio by using the model brightness distribution of JSR. We construct the equatorial brightness distribution model and obtain the relation between the dawn-dusk ratio and neutral wind velocity. Estimated neutral wind velocity is 46 +/- 11 m/s, which reasonably corresponds to the numerical simulation of Jupiter's upper atmosphere (Tao et al., 2009). In order to explain short term variations of the dawn-dusk ratio (the third result), we examined the effect of the global convection electric field driven by tailward outflow of plasma in Jupiter's magnetosphere. As the result, it is suggested that typical fluctuation of the convection electric field strength was enough to cause the observed variations of the dawn-dusk ratio. It is also confirmed that some magnetospheric plasma parameters indicated the existence of substorm like event during the observation period. Hence, these results imply that fluctuations of tailward outflow affect Jupiter's deep inner magnetosphere.

### Reference

- Brice, N. M. and T. R. McDonough, *Icarus*, 18, 206-219, 1973.  
Tao, C. et al., *J. Geophys. Res.*, 114, A8, 2009.  
Tsuchiya, F. et al., *J. Geophys. Res.*, 116, A09202, 2011.

Keywords: Jupiter, Magnetosphere, Radiation Belt, Synchrotron Radiation, Radio Interferometer



## Ground based multispectral imaging observation of Saturn's large storm

HAMAMOTO, Ko<sup>1</sup>, TAKAHASHI, Yukihiro<sup>1\*</sup>, Makoto Watanabe<sup>1</sup>, WATANABE, Shigeto<sup>1</sup>, FUKUHARA, Tetsuya<sup>1</sup>, SATO, Mitsuteru<sup>1</sup>

<sup>1</sup>Department of CosmoSciences, Graduate School of Science, Hokkaido University

Storms occur regularly in Saturn's atmosphere. Large storms called as Great White Spots(GWSs), which are about ten times larger than regular storms (300-3000 km in diameter), and occur about once per Saturnian year (29.5 Earth years). It is difficult to observe deep Saturn's atmosphere directly because Saturn's surface layer is covered by optically thick clouds. Observation of GWSs is one of the few method to get information about convective activity of Saturn's deep atmosphere [Hueso and Sanchez-Lavega, 2004]. In early studies, cloud structure of GWSs was estimated by radiative transfer calculation using images at several wavelengths in methane absorption bands [Acarreta and Sanchez-Lavega, 1999]. However, paucity of wavelengths in methane band have possibility to lead to ill-constrained cloud model parameters.

A new storm was detected on 5 December 2010, earlier than expected timing inferred from previous storm period by about ten years. The storm happened as a visible bright spot on northern hemisphere of Saturn (northern latitude of 37.7 degrees), and two weeks later, it's west-east size expanded 15,000 km. About two months after, it encircled the planet. This storm was observed by Cassini spacecraft. Cassini's images using three narrow bandpass filters (center wavelengths are 727, 750, 889 nm) showed horizontal variation of brightness at these wavelengths [Fischer et al., 2011]. However, the detail spectral information of the storm is still unknown. And also there is no comparison of spectrums in different periods.

In this study, an observation of the Saturn's storm used Multi-Spectral Imager(MSI) and a ground-based 1.6 m reflector named Pirka telescope operated by Hokkaido University. MSI, which uses two Liquid Crystal Tunable Filters(LCTF) and an EM-CCD, was developed in Hokkaido University and enabled us to capture spectral images in a short time. Spectral imaging data of the storm, in the wavelength range of 400-1100 nm with FWHM of 5-10 nm, at 180 colors, were obtained within 30 minutes on 5 May 2011. Additionally on 6 June 2011, we observe Saturn in three methane bands at 88 colors.

We succeeded in deriving latitudinal variation of Saturn's spectrum in visible and near-infrared range. Methane absorption bands were confirmed and the rough shape of the spectrum is consistent with past observations [ex. Karkoschka, 1994]. And center-limb profile of spectrum at same latitude have possibility to provide characteristic of scattering, because of less longitudinal variation of spectrum. In addition, we drew a comparison between latitudinal variation of Saturn's absolute reflectivity in three methane absorption bands on 5 May and 6 June. In these datas, the reflectivity slightly changed In about a month. This period is fading phase of this GWS. Therefore detection of an absolute reflectivity variation at the latitude of the GWS lead to a fading speed information of the GWS. And a reflectivity of Saturn after the GWS fade outed is also important in terms of an influence on static cloud level by the GWS. Therefore, we are scheduled to observe Saturn in spring of 2012.

In future works we will observe Saturn's atmosphere regularly to derive temporal variation of spectrums and cloud structure using Pirka telescope.

Keywords: Saturn, great white spot, ground based observation, spectrum

## De effect on Jupiter's decametric non-Io-A source

IMAI, Kazumasa<sup>1\*</sup>, FUKUSHIMA, Koichi<sup>1</sup>, UJIHARA, Akiya<sup>1</sup>, IMAI, Masafumi<sup>2</sup>

<sup>1</sup>Department of Electrical Engineering and Information Science, Kochi National College of Technology, <sup>2</sup>Department of Geophysics, Graduate School of Kyoto University

One of the unresolved problems of Jupiter's decametric radio emissions is the variation of occurrence probability on the order of a decade. The variation was first thought to be due to changes in solar activity (solar cycle). The Sun can influence the detection of Jovian decametric radiation by changing the local observing conditions, changing the density of plasma in the interplanetary medium and by changing conditions at the Jupiter radio source.

The period of the variation was also close to the orbital period of Jupiter (11.86 years). Carr et al. [1970] showed that such variations are closely correlated with the Jovicentric declination of the Earth (De). The range of the smoothed variation of De is from approximately +3.3 to -3.3 degrees. If this is the case, the observed variation appears to be a purely geometric effect caused by changes in the beam cross section seen from the Earth. The shape and angular dimensions of the part of the emission beam accessible to the Earth is shown in Figure 6a in Carr et al. [1970]. However the detail of the beam model has not been proposed so far.

Garcia [1996] extensively studied and confirmed this De effect. The radio observations used in this study were mainly taken by Yagi antennas located at the University of Florida Radio Observatory (UFRO). The occurrence probability of the non-Io-A source varies in close step with De. Garcia [1996] reports that the changes in source width and location for non-Io-A are very large over the roughly 7 degree range of De. The high CML edge of the non-Io-A source also has a very strong dependence on De.

We show the long-term periodic variation of the occurrence probability of Jupiter's decametric radio emissions is caused by the De effect which is related to the pure geometrical effect of sharp radio beaming. We propose the searchlight beam model which can explain this sharp beaming especially in a latitudinal direction. The three dimensional structure of the radio source is the important key parameter to produce the searchlight beam of Jupiter's decametric radio emissions. We calculate the beam pattern by using the dimensions of the radio coherent region. The calculated results show the existence of sharp beaming in the latitudinal direction. As the searchlight beam is the intensified part of a conical sheet beaming toward the equatorial plane, it does not conflict with the previous idea of the conical sheet model. We also propose the delta zone effect to explain the cyclic changes of CML and the effective width of the non-Io-A source. We believe that the searchlight beam model is very important in understanding the beaming of the planetary radio emissions.

### References

Carr, T.D., A.G. Smith, F.F. Donovan, and H.I. Register, The twelve-year periodicities of the decametric radiation of Jupiter, *Radio Sci.*, 5, pp.495-503, 1970.

Imai, K., L. Garcia, F. Reyes, M. Imai, and J.R. Thieman, A Model of Jupiter's decametric Radio emissions as a searchlight beam, *Planetary Radio Emissions VII*, edited by H.O. Rucker, W.S. Kurth, P. Louarn, and G. Fischer, Austrian Academy of Sciences, Graz, Austria, pp.179-186, 2011.

Keywords: Jupiter Radio, decametric wave, beam structure, De effect, radio source, radio emission mechanism

## 1 micro-m camera IR1 onboard AKATSUKI: Current status and results of observations

OHTSUKI, Shoko<sup>1\*</sup>, IWAGAMI, Naomoto<sup>2</sup>, SATOH, Takehiko<sup>1</sup>

<sup>1</sup>ISAS/JAXA, <sup>2</sup>University of Tokyo

"Akatsuki" spacecraft which has launched by the Japan Aerospace Exploration Agency in 2010 is keep cruising to Venus for 2015. The results of the imaging carried out by IR1 camera onboard "Akatsuki" during the cursing phase after the Venus fly-by in December 2010 are described.

The images taken by IR1 in 2011 are followings.

- (1) Photometry of the dayside of Venus from a distance of over 10 million kilometers in March 2011
- (2) Star imaging to check the change of the absolute sensitivity.
- (3) Deep space imaging to check the normal operation of the camera after perihelion.

The phase curve of Venus at 0.90 micrometer covering phase angle from 1 deg to 56 deg has been obtained by the photometry observations of Venus. Simultaneous analysis with the phase curve at 2.02 micrometer by 2 micron camera IR2 onboard "Akatsuki" constrains cloud model of Venus.

Current status and problems of detector are also discussed based on images of star and operation tests.

Keywords: AKATSUKI, near infrared, Venus atmosphere, phase curve, cloud particle

## A model to study the Venus cloud structure based on several Venus observations, wherein SOIR solar occultations on Venus

TAKAGI, Seiko<sup>1\*</sup>, IWAGAMI, Naomoto<sup>1</sup>, Arnaud Mahieux<sup>2</sup>, Valerie Wilquet<sup>2</sup>, AnnCarine Vandaele<sup>2</sup>

<sup>1</sup>Graduate School of science, the Univ. of Tokyo, <sup>2</sup>Belgian Institute for Space Aeronomy

Venus is our nearest neighbor, and has a size very similar to the Earth's; however, previous spacecraft missions discovered an extremely dense (92 bar at the surface) and CO<sub>2</sub>-rich atmosphere, with H<sub>2</sub>SO<sub>4</sub> clouds located at altitudes between 40 and 70 km. These clouds cover the whole planet.

A cloud model was proposed by Pollack et al. (1993), with a vertical distribution of optical thicknesses of the different cloud particles (modes 1, 2 and 3). However, this model might be improved using new data obtained in the recent past from ground-based observations (IRTF telescope in Hawaii) and in-situ measurements from spacecraft observations (SOIR on Venus Express).

A new cloud model, correcting for some Pollack model's problems, is proposed using data from previous entry probes [Takagi & Iwagami, 2011]. However, this model does not describe the global Venus cloud structure.

The purpose of this work is to construct a more realistic cloud model. Ground-based spectroscopic observations of the Venus low-latitude region and Venus Express/SOIR observations of high-latitude will be used to construct this new cloud model.

Keywords: Venus, cloud, Venus Express, SOIR

## Venusian cloud structure in the northern high-latitude region estimated from VEX/VIRTIS-H data

KURODA, Morihiro<sup>1\*</sup>, KASABA, Yasumasa<sup>1</sup>, MURATA, Isao<sup>2</sup>, NAKAGAWA, Hiromu<sup>1</sup>, Pierre Drossart<sup>3</sup>

<sup>1</sup>Graduate School of Science, Tohoku University, Department of Geophysics, <sup>2</sup>Graduate School of Environmental Studies, Tohoku University, <sup>3</sup>LESIA, Observatoire de Paris, Meudon, France

This paper presents the characteristics of northern high-latitude cloud, i.e., its opacity, cloud top temperature and altitude, and these relationships estimated from Venus Express (VEX) observations.

Venusian clouds mainly consist of sulphuric acid droplets in the altitude of 40-70 km. Recent long-term observations by Venus Monitoring Camera (VMC) and Visible and Infrared Thermal Imaging Spectrometer - M channel (VIRTIS-M) aboard VEX has investigated the south polar vortex [e.g., Luz et al., 2011]. For an example, the lower cloud top altitude at southern polar region is reported [Ignatiev et al., 2008]. We investigated the cloud structure in these regions by the data observed by VIRTIS - High spectral resolution channel (VIRTIS-H), which can get information of northern hemisphere that has not been well reported by VMC and VIRTIS-M. We compared these characteristics with previous reports for the Southern hemisphere, and investigate the opacity, cloud top temperature and altitude, and these relationships between them.

(1) In the 2.3 $\mu$ m thermal radiation from the night side, we could not find enough flux from the region more than 70degN in latitude. In the study combined to a radiation transfer analysis, the cloud optical thickness in high latitude region is constantly about twice of that in lower latitudes. It suggests that the clouds in polar region are thicker or has different aerosol characteristics.

(2) We retrieved the cloud top temperature from 5 $\mu$ m radiation and the cloud top altitude by 2.2 $\mu$ m CO<sub>2</sub> absorption band. The averaged cloud top temperature increased from 75degN to North Pole. On the other hand, the averaged cloud top altitude at 80degN (65.4 $\pm$ 0.7 km) was lower than that at 50 degN (69.3 $\pm$ 0.5km). This is consistent with the characteristics in the southern hemisphere [Ignatiev et al., 2008]. In an event study, it was also shown that the cloud top altitude in the cold collar regions surrounding the hot polar vortex is  $\sim$ 1km higher.

(3) We retrieved the averaged latitudinal distributions of cloud opacity, cloud top temperature and altitude in the northern hemisphere from 15 orbits nadir observations, with the resolution of 1 deg. in latitude. There was a negative correlation between the cloud top temperature and its altitude. No other correlations were not clear.

In the paper, we will report the results with the discussion on their interpretations.

Keywords: venusian atmosphere, polar vortex, cloud top altitude, cloud top temperature, cloud optical depth

## Venusian wind velocity distributions in middle-to-high latitude regions derived from the UV/IR images observed by Venus

SATO, Mizuki<sup>1</sup>, MURATA, Isao<sup>2\*</sup>, KASABA, Yasumasa<sup>1</sup>, KOUYAMA, Toru<sup>3</sup>

<sup>1</sup>Dept. of Geophysics, Tohoku Univ., <sup>2</sup>Environmental Studies, Tohoku Univ., <sup>3</sup>EPS, Univ. of Tokyo

We tried to derive the wind velocity distribution in the southern high latitude regions of Venus using the UV images taken by the Venus Monitoring Camera (VMC) on Venus Express (VEX). We focused on the longitudinal distributions of wind velocity, and found a possible correlation between the distributions of cloud-top temperature and meridional wind.

The UV images of Venus has contrasting distributions. They have been thought to show the distributions of unknown UV absorber which exists in the altitude of approximately 70km around the cloud top where the wind vectors have been estimated by tracking the cloud motions.

In addition, we can estimate the cloud top temperature from the brightness images in the mid-infrared region. The atmospheric vortices on both polar regions have been observed, and the vortices are made of two parts; one is high temperature regions near the pole called "polar dipole", and the other is low temperature regions called "polar collar" outside of the dipole. The dipoles have a structure with the wave-number of two and rotate with the period of 2 to 2.5 days. The collars have a crescent structure with the wave-number of one and the phase fixed to the local time.

It is suggested that there is a correlation between the distributions of temperature and wind velocity. For example, the adiabatic heating due to a descending flow has been pointed out as a possible cause of the dipole. Indeed, poleward meridional winds have been found at the limbs of the vortices by observations in the UV region [Sanchez-Lavega et al., 2008; Moissl et al., 2009].

In this study, we aimed to derive the wind velocity distribution by tracking UV cloud images in middle-to-high latitude taken by VMC, and examine the correlation between the longitudinal distribution of temperature seen in the IR region and wind velocity seen in the UV region.

We adopted the cloud tracking method developed by Kouyama et al. (2009) for the detection of wind fields in high latitude regions. We modified this method to achieve the cloud tracking in high latitude regions where the tracking was hard. We got the result of wind velocity consistent with Kouyama et al. (2009) in middle-to-low latitude.

To get the wind velocity fields with respect to the dipole, we need to define a coordinate system fixed in the dipole. We fitted an ellipse to the dipole in mid-IR region and derived the distribution of wind velocity on the basis of its long axis. We analyzed data obtained from 5 orbits. The results show that there is no clear longitudinal distribution for zonal wind. In contrast, we found the structure which can be approximated to the zonal wavenumber of two in the meridional wind velocity. It suggests that we can approximate the streamline of wind by a dipole-like ellipse.

However, there is a difference in the longitudinal phase between the dipole in temperature and meridional wind structure. In addition, there is a significant variation in the phase difference with a period of as short as about 1 day. This result suggests that the longitudinal structure of the dipole is not made by wind steadily, and we need to consider the possibility that the dipole is made by another factors such as the wave phenomena. We need some additional analyses mainly to track the time variation of the phase difference.

Keywords: Venus, Polar vortex, Wind velocity, Longitudinal distribution, Venus Express, Venus Monitoring Camera



## Westward acceleration of the mesospheric and thermospheric atmosphere in Venus caused by gravity waves

HOSHINO, Naoya<sup>1</sup>, FUJIWARA, Hitoshi<sup>2\*</sup>, TAKAGI, Masahiro<sup>3</sup>, KASABA, Yasumasa<sup>1</sup>

<sup>1</sup>Dep. Geophysics, Tohoku Univ., <sup>2</sup>Fac. Sci. Tech., Seikei Univ., <sup>3</sup>Dep. Earth and Planetary Science, Univ. Tokyo

We present the numerical simulations for the investigation of the effects from gravity waves to the Venusian mesosphere and thermosphere dynamics. The results reproduced the fast westward wind acceleration above 90 km in altitude. The result first showed that westward acceleration at 110km occurs mainly in the nightside.

Momentum transport from the cloud layer (50-70km) toward the upper atmosphere by gravity waves is essential to understand the circulation in the Venusian mesosphere (70-110km) and thermosphere (>110km) (e.g. Bougher et al. [2006]). Zhang et al. [1996] performed simulations with a gravity wave parameterization and showed that the momentum transport by gravity waves drove the retrograde zonal wind (RZW) as fast as 15 ? 30 m/s above about 140 km. They also showed the westward shift of the O<sub>2</sub>-1.27 $\mu$ m nightglow emission region because of the RZW.

We use the parameterizations which can consider the wave-wave interaction and the attenuation of gravity waves caused by molecular viscosity. We introduced these physical processes by using the new gravity wave parameterization developed by Medvedev et al. [2000] (Medvedev scheme) into our GCM calculation, which enabled us to investigate the effects of gravity waves on the Venusian mesosphere and thermosphere.

In the Medvedev scheme, the characteristic horizontal wavelength and the spectrum of the vertical wavelength at the lower boundary are the adjustable parameters. For the former, it is set to be 500 km [Kasprzak et al. 1988] in this calculation. For the latter, we assume the Desaubies spectrum, which is the familiar spectrum shape of the terrestrial gravity waves, at the lower boundary. In this calculation, the wind velocity distribution at the lower boundary (80 km) is the solid body rotation with the equatorial wind velocity of 40 m/s.

The result shows that gravity waves, which transport the westward momentum upward, drive the RZW above about 90 km. The strength of the RZW becomes stronger with height in the 90-125 km region. The maximum RZW velocity is about 120 m/s at about 125 km. The RZW velocity is weaker with the height in the 125-140 km region and becomes constant (about 60 m/s) above about 140 km. The vertical change of the RZW strength is interpreted as the result of the wave filtering caused by the background wind.

We also first showed that in the horizontal wind velocity distribution at about 110 km, where wind velocity is observed with the CO and CO<sub>2</sub> absorption/emission lines, the westward acceleration caused by gravity waves occurs mainly in the nightside. On the other hand, the subsolar-to-antisolar flow is dominant in the dayside in spite of the existence of the RZW.

(This paper will be submitted to J. Geophys. Res.)

Keywords: Venus, GCM, mesosphere and thermosphere, wind velocity field, gravity wave

## X-ray observation from Venus upper atmosphere by HINODE

KANAO, Miho<sup>1\*</sup>, YAMAZAKI, Atsushi<sup>1</sup>, KOUYAMA, Toru<sup>1</sup>, NAKAMURA, Masato<sup>1</sup>

<sup>1</sup>ISAS/JAXA

Venus transit across the Sun will occur on 5 June, 2012. X ray is emitted by the charge exchange of the high charge state solar wind ions due to electron capture from Venus corona. In this study, the X-ray emission from Venus corona is estimated and the possibility of the observation by HONODE satellite is discussed.

The solar wind ions impact on the ionspheric particles happens to charge exchange to result into the excited emission. Emission lines of charge exchange are 1.7-2.21nm of O<sup>7+</sup>, 2.7-4.1nm of C<sup>6+</sup>, 2.6-3.38 nm of C<sup>5+</sup>. We estimated that the intensity of the charge exchange emission is totally estimated  $2.30 \times 10^{-7}$  photons/cm<sup>2</sup>/sec at limb. The X-ray emissions from Venus corona will be detected by observation for at least 13 hours. Venus nightside X-ray image let us know the distribution of the neutral corona.

The solar wind particle induced to the ionosphere has asymmetry with north and south direction. The short length band of EIS includes 18.4nm emission lines of O<sup>6+</sup> charge exchange and 19.3nm emission line of O<sup>7+</sup>. The emission of 18.4nm(O<sup>6+</sup>) is  $1.51 \times 10^{-7}$  photons/cm<sup>2</sup>/sec and the luminosity is 6.8W.

Keywords: Venus, upper atmosphere, HINODE

## Response of the Martian thermosphere to the EUV flux enhancement during solar flare events with a GCM

ICHIKAWA, Yoshinori<sup>1</sup>, FUJIWARA, Hitoshi<sup>2</sup>, KASABA, Yasumasa<sup>1\*</sup>, TERADA, Naoki<sup>1</sup>, TERADA, Kaori<sup>1</sup>, HOSHINO, Naoya<sup>1</sup>

<sup>1</sup>Dept. Geophys. Tohoku Univ., <sup>2</sup>Faculty of Science and Technology, Seikei University

The Martian oxygen corona in the exosphere consists of non-thermal oxygen atoms ( $O^*$ ) produced mainly by the dissociative recombination of  $O_2^+$  ions produced in the lower thermosphere/ionosphere. The dissociative recombination is the major process of the Martian atmospheric escape in the present solar condition. This means that, in order to calculate the accurate escape flux of  $O^*$ , it is needed to understand not only the spatial distribution of  $O^*$  in the exosphere but also the behavior of  $O_2^+$  in the thermosphere/ionosphere. Many researchers have indicated the dependence of temperature, wind, and composition distributions in the Martian upper atmosphere on long-term variations of the solar EUV flux e.g. solar maximum-to-minimum activities [e.g., Bougher et al., 1991]. Recently, observations by Mars Global Surveyor (MGS) indicated that the Martian lower ionosphere varied significantly in association with enhancement of the solar X-ray and EUV flux range during a solar flare [Mendillo et al., 2006]. It may suggest that the Martian thermosphere also vary largely in association with short-term variations of the solar X-ray and EUV flux. It is also shown time-dependence of terrestrial planet thermospheres on instantaneous variations of the solar EUV flux [Bougher et al., 1999]. This work indicates that time-dependent of each planet thermosphere are different because of difference of main cooling processes. Moreover, it is indicated that temperature of the past Martian thermosphere was much larger, because the solar X-ray and EUV flux of the early sun was more powerful [Vaille et al., 2010]. Solar flares were also more powerful in the early sun, so response of the Martian thermosphere to short-term variations of the solar X-ray and EUV flux may be different from that of the solar X-ray and EUV flux in the present solar condition.

In this study, we investigated response of the Martian thermosphere to the short-term variations of the solar X-ray and EUV flux with a Martian Global Circulation Model.

1. This Martian GCM calculates enhancements of the temperature and scale height at the sub-solar point of the exobase by about 42 K and 13 km, respectively, when the solar X-ray and EUV flux (1-20 nm) increases 60 times as much as the usual one for an hour. In this study, variations of the global mean temperature and scale height were 80 K and 27 km, respectively, during a solar cycle. This means that the temperature and scale height of the Martian upper atmosphere would increase by about 50 % during a big solar flare event even in the present condition.

2. This Martian GCM calculates enhancements of the temperature at the sub-solar point of the exobase by about 20 % (42 K) for 2 hours, and it takes 9 hours to decrease to the value of steady state. On the other hand, the Venusian GCM, which was updated by changing the Martian parameter to Venusian parameter, calculates enhancements of the temperature at the same point by about 31 % (63 K) for 1.25 hours, and it takes 3 hours to decrease to the value of steady state. This means that increasing rate of temperature of Venusian thermosphere is larger than that of Martian thermosphere, while time variation of the Venusian thermosphere to the solar X-ray and EUV flux enhancement is shorter than that of Mars, because of difference of main cooling processes.

3. This Martian GCM produces the Martian thermosphere when solar X-ray and EUV/UV flux increases between twice and 20 times. In this state, we simulate the same solar X-ray and EUV flux enhancement of the present sun's flare. This model calculates enhancements of the temperature at the sub-solar point of the exobase by about 59 % (205 K). This means that effects of solar flares in the early sun on the Martian thermosphere might be larger 3 times than that in the present solar condition.

Keywords: Mars, thermosphere, solar flare, Venus

## Examination of Orbiters for Martian Atmospheric Escape Study

MATSUOKA, Ayako<sup>1\*</sup>, ABE, Takumi<sup>1</sup>, ISHISAKA, Keigo<sup>2</sup>, KUMAMOTO, Atsushi<sup>3</sup>, KURIHARA, Junichi<sup>4</sup>, SEKI, Kanako<sup>5</sup>, TAGUCHI, Makoto<sup>6</sup>, TERADA, Naoki<sup>7</sup>, FUTAANA, Yoshifumi<sup>8</sup>, YAGITANI, Satoshi<sup>9</sup>, YAMAZAKI, Atsushi<sup>1</sup>, YOKOTA, Shoichiro<sup>1</sup>, SAKANOI, Takeshi<sup>3</sup>, NAKAGAWA, Hiromu<sup>7</sup>, Martian Atmospheric Escape Study Group<sup>1</sup>

<sup>1</sup>ISAS/JAXA, <sup>2</sup>Toyama Pref. Univ., <sup>3</sup>Planet. Plasma Atmos. Res. Cent., Tohoku, <sup>4</sup>Cosmosciences, Hokkaido Univ., <sup>5</sup>STEL, Nagoya Univ., <sup>6</sup>Rikkyo Univ., <sup>7</sup>Dept. Geophys., Grad. Sch. Sci., Tohoku, <sup>8</sup>IRF, Sweden, <sup>9</sup>Kanazawa Univ.

The atmospheric escape from Mars is considered to be closely associated with the evolution of the Martian atmosphere as well as the existence of the water on Mars. We are now investigating a project to study the global feature and the physical process of the atmospheric escape from Mars. It is expected to consist of at least two orbiters; one of the orbiters is aimed to make in-situ observation of plasma and thin atmosphere at about 100 km altitude, and the other is for the atmospheric imaging and solar-wind monitor. We are planning to make simultaneous observation of the atmospheric escape by the interaction with the solar wind by both of in-situ measurement orbiter and remote-sensing one. Now we are examining the quantitative measurement targets to fully understand the Martian atmospheric escape. At the same time, the sorts and performance of scientific instruments on these orbiters are examined. And furthermore, the preliminary spacecraft design, orbit design and mission plan to achieve the scientific goal are investigated.

Keywords: Mars, Atmospheric escape, Planetary exploration, Solar wind

## Feasibility study of Mars' wind observation from a satellite orbit using a sub millimeter wave sounder

KOBAYASHI, Tomonori<sup>1\*</sup>

<sup>1</sup>Graduate School of Engineering, OPU

In order to know the atmosphere circulation of Mars, there is a need to know the distribution of wind speed on Mars. By observing Doppler shifts of molecular emission spectra of the Martian atmosphere, vertical profiles of wind speed in the Martian middle/upper atmosphere can be measured. In this study, we present a feasibility study of Martian wind measurement using a submillimeter sounder from an orbiting platform. The spatial and time resolutions achievable by submillimeter wave observations from Martian orbits are investigated.

Keywords: submillimeter wave, doppler shift, mars, wind

## Progress of the SPART project to monitor planetary middle atmospheres

MORIBE, Nayuta<sup>1\*</sup>, MAEZAWA, Hiroyuki<sup>2</sup>, KONDO, Syusaku<sup>3</sup>

<sup>1</sup>Graduate School of Science, Nagoya Univ., <sup>2</sup>School of Science, Osaka Prefecture Univ., <sup>3</sup>Solar-Terrestrial Environment Lab., Nagoya Univ.

Investigating the abundance and time variation of minor constituents and their isotopes provide us an important information about the dynamical and chemical balances and evolutionary processes of planetary atmospheres. To study how activities of the Sun, a typical G-type star in our galaxy, influence the physical conditions and (photo) chemical reaction network of the atmospheres of Venus, Mars and gas-giant planets, we have promoted regular and long-term observations of these planetary middle atmospheres at 90 ? 345 GHz bands developing a 10-m ground-based Solar Planetary Atmosphere Research Telescope (SPART).

In November 2011 we succeeded first detection toward Mars and mapping observation toward Orion Molecular Cloud 1 with a spectral line for rotational transition of carbon monoxide (J=1-0: 115 GHz) by using the SPART. Now we are just starting to carry out test regular observations. In this talk the current status of this project will be presented.

Keywords: millimeter wave, submillimeter wave, planet, middle atmosphere, solar system, ground-based telescope



## Mercury's sodium tail distribution and the source processes of the exosphere

FUSEGAWA, Ayaka<sup>1\*</sup>, KAMEDA, Shingo<sup>1</sup>, DAIROKU, Hayato<sup>1</sup>, KAGITANI, Masato<sup>2</sup>, OKANO, Shoichi<sup>2</sup>

<sup>1</sup>Rikkyo University, <sup>2</sup>Tohoku University

Mercury has a thin atmosphere. In the past, Mercury has been observed by Mariner 10 and MESSENGER, and ground-based observations have also been carried out. H, He, O, Na, Mg, K, and Ca were detected in its atmosphere. Solar-photon-stimulated desorption, sputtering by impacting solar particles, and meteoroid vaporization are considered to be the source processes of Mercury's exosphere. However, the primary process among these three processes is unknown as yet. Sodium atoms are excited by the energy from sunlight, and they return to the ground state by emitting energy isotropically. The resonance scattering constitutes exospheric sodium emission. This emission well suited for study by ground-based observations because of its high intensity. The sodium atoms are accelerated in the anti-sunward direction due to their isotropic scattering. This is called sodium tail. Past observations have shown that the intensity distribution of exospheric sodium emission changes with time. This study aims to make ground-based observations of exospheric sodium emission, to determine the distribution of the sodium tail, and to consider the source processes of Mercury's exosphere.

We have observed Mercury's sodium exosphere at the Haleakala Observatory since April 2011. The observations were made using a 40 cm Schmidt-Cassegrain telescope, a high-dispersion spectrograph, and a CCD camera. In this term, the telescope system at the Haleakala Observatory was remotely-operated in Japan. At this observation, the slit of spectrograph was set on Mercury, and its direction was set parallel to the anti-sunward direction. The slit width is 2.5 arcsec, and apparent diameter of Mercury was from 5.0 to 10.4 arcsec. The sodium distribution was scanned by changing slit position. Exposure time was 50 second, and it took 30 minutes to get a whole image of the sodium tail.

We analyzed observational data collected from April 27, 2011, to May 30, 2011, and from June 24, 2011, to August 5, 2011. The observation times were from Mercury rise to before sunrise in the former observation period, and from just after sunset to Mercury set in the latter observation period. We determined the intensity distribution of exospheric sodium emission by using the observational data. We compared the intensity distributions on May 18, June 24, and July 1. These distributions have two characteristics. The first is temporal variation of the intensity of sodium emission from the equator of Mercury changed. The second is the emission from the northern part of Mercury was not detected on June 24.

In this study, we discuss the variation of the sodium emission of the equator of Mercury changed. Sputtering by impacting solar particles, one of the source processes of Mercury's exosphere, is that solar wind ion arrives at the surface of Mercury from cusp region of Mercury's magnetosphere. So we think that change of solar wind magnetic field causes change of variation of the sodium distribution. The magnetic reconnection in the case of northward interplanetary magnetic field is different in the case of southward interplanetary magnetic field. This causes change place where solar wind ion arrives at the surface of Mercury. We compared our observational data with the data of solar wind magnetic field observed by MESSENGER. In this presentation, we discuss between the sodium distribution and the variation of solar wind magnetic field.

Keywords: Mercury, Sodium, Ground-based observation

## Interaction between solar wind and mini-magnetosphere

NAKAMURA, Masao<sup>1\*</sup>

<sup>1</sup>Osaka Prefecture University

Interaction between the solar wind and the mini-magnetosphere of dipolar magnetized objects is investigated by a three-dimensional hybrid simulation, which treats the ions as kinetic super particles via particle-in-cell method and the electrons as a massless fluid. The hybrid simulation is suitable for the study of the mini-magnetosphere which scale is the order of the ion Larmor radius of the solar wind ions at the magnetopause boundary, because the ion kinetic effects are important for its structure. In the northward interplanetary magnetic field (IMF) condition, the shape of the mini-magnetosphere is similar to a down-sized geomagnetosphere. However cusp reconnection twists the field lines over of the cusp region due to the Hall effects. In the southward IMF condition, patchy reconnection is generated in the dayside magnetopause boundary and generates plasmoids or Flux Transfer Events as large as a quarter of the magnetosphere. We will discuss the boundary structures of the mini-magnetosphere.

Keywords: Interaction between solar wind and mini-magnetosphere, 3D hybrid simulation

## Estimation of OI 630nm emission from Enceladus torus by various process

KODAMA, Kunihiro<sup>1\*</sup>, KAGITANI, Masato<sup>1</sup>, OKANO, Shoichi<sup>1</sup>

<sup>1</sup>Geophys. Sci., Tohoku Univ.

It has been known that there are H<sub>2</sub>O molecules and their dissociative products. Cassini mission discovered plume on Saturn's icy moon, Enceladus. And this small moon supplies molecules and ice grains to the Saturn's magnetosphere. This materials distribute like a torus, so called enceladus torus. If we can monitor distribution and time variation of the Enceladus torus continuously, we can get more clear understanding about Saturn's magnetosphere and its variability. In order to accomplish remote-sensing of the Enceladus for a long period, we made ground-based observation of OI 630nm emission of the Enceladus torus at Haleakala observatory.

We successfully detected the line emission with 1200 minutes total exposure time by ground-based observation carried out in Mar. 2011. In order to derive physical information, we must clear what process cause this emission. We had assumed that main process for this emission is electron impact excitation. But other process is also existing, photo dissociation of H<sub>2</sub>O and OH.

In this presentation, I will report the contribution of non electron impact excitation process.

Keywords: Saturn, Enceladus, ground-based observation, emission, neutral

## Electron density observations from Cassini RPWS in the Enceladus torus

ODANAKA, Ena<sup>1\*</sup>, OKANO Shoichi<sup>1</sup>, OBARA Takahiro<sup>1</sup>, MOROOKA Michiko<sup>2</sup>

<sup>1</sup>Planet. Plasma Atmos. Res. Cent., Tohoku Univ., <sup>2</sup>Swedish Institute of Space Physics

One of Cassini's most exciting results is a detection of a plume which expels water vapor and ice grains from south pole of the moon Enceladus [Dougherty et al., 2006; Spahn et al., 2006; Porco et al., 2006; Waite et al., 2006]. This water creates an extended torus around Saturn. A large amount of gas is ionized within the plume and becomes the major source of plasma for E ring and Saturn's magnetosphere. The inner magnetosphere consists of a dense and cold plasma in the shape of a disk [Persoon et al., 2005]. Recently, observations from Cassini Radio Plasma Wave Science (RPWS) revealed the presence of dusty plasma and indicate the interaction between plasma disc and dusty plasma E ring [Morooka et al., 2011]. However, these observations were only near Enceladus. We investigate the plasma distribution on Enceladus orbit. We use Cassini RPWS data and analyze the electron densities in the Enceladus torus, and plan to analyze the azimuthal distribution of Enceladus.

## Characteristics of the transient evolution of the auroral acceleration region of Saturn derived from radio spectra

MARUNO, Daichi<sup>1\*</sup>, KASABA, Yasumasa<sup>1</sup>, KIMURA, Tomoki<sup>2</sup>, MORIOKA, Akira<sup>1</sup>, CECCONI, Baptiste<sup>3</sup>

<sup>1</sup>Tohoku University, <sup>2</sup>ISAS, JAXA, <sup>3</sup>LESIA, Observatoire de Paris

We show the preliminary result for the characteristics of the altitude profile variation seen in the lower- frequency extensions of Saturn kilometric radiation (SKR) associated with substorm-like events.

SKR is an intense radio emission with a peak frequency between 100 and 400 kHz. It is thought to be emitted from energized electrons accelerated along auroral field lines via the Cyclotron Maser Instability (CMI) [Wu and Lee, 1979]. Compared with Earth and Jupiter, SKR shows several unique characteristics such as the modulation at or close to the planetary rotation period [Desch and Kaiser, 1981], long-term variation of modulation period [Galopeau and Lecacheux, 2000], North - South asymmetry of modulation period [Gurnett et al., 2009].

During the high activity of SKR, It is commonly seen that SKR expands toward lower frequency. It can be interpreted as an expansion of the auroral acceleration region to higher altitude with weaker magnetic field strength because SKR is emitted at approximately local electron cyclotron frequency. Similar characteristics have been known in the terrestrial auroral kilometric radiation (AKR) for a long time. For example, using this characteristic in AKR frequency variations, Morioka et al. [2010] derived the two-step evolution model of the auroral acceleration region during substorms. Our motivations are to adopt similar analysis to Saturn and to compare auroral field line accelerations between two planets.

In a previous study, Jackman et al. [2009] reported the general relationship between the lower-frequency extensions of SKR and substorm-like events seen as plasmoids in the magnetotail. We focus on short variations of such phenomena, from several minutes to hours. We use SKR spectra data observed from Cassini/RPWS high frequency receiver (HFR). Its high time resolution, approx. 15 sec, is enough to show that the time scale of lower-frequency extension of SKR, several hours, longer than that of AKR. In this case, we should consider not only the visibility effect (i.e., beaming at the source and propagation along the light-path from the source) but also the unique enhancement due to the rotation of SKR sources. In order to reduce the former effect, we use the data when Cassini locates specific position (in this preliminary study, radial range from 10 to 100 Rs, latitudinal range from -5 to +5 degrees, SKR phase range from -45 to +45 degrees). Based on this analysis, we now try to grasp (1) the relationship of maximum/minimum/central frequency of SKR versus its total flux (as a proxy effect from the amount of field-aligned current), and (2) the relation of maximum/minimum/central frequency of SKR versus specific SKR phase (as a proxy effect from the rotational enhancement). These characteristics will be used for event studies of short-term evolution of auroral acceleration region during substorm-like events.

Keywords: Saturn, SKR, Cassini/RPWS

## Simulation study of the current-voltage relationship of the Io tail aurora

MATSUDA, Kazuya<sup>1\*</sup>, TERADA, Naoki<sup>1</sup>, KATOH, Yuto<sup>1</sup>, MISAWA, Hiroaki<sup>1</sup>

<sup>1</sup>Department of Geophysics, Graduate School of Science, Tohoku University

Subcorotation of Iogenic plasma in the Io plasma torus has been understood as electric drift by a perpendicular electric field with respect to the Jovian magnetic field. It has been considered that a part of the radially integrated electric field would be imposed along the magnetic field lines and would cause the Io's trailing tail aurora. Observations have been shown that the Io tail aurora extends for approximately 100 degrees downstream in longitude from the Io's magnetic footprint. It remains unresolved why the precipitating electron energy corresponding to the voltage is constant with longitude despite the decreasing parallel current density. The purpose of this study is to clarify how the current-voltage relationship of the Io tail aurora realizes.

We applied a semi-discrete central scheme to extended multi-magneto-fluid equations which include the electron convection term and investigated the relationship between a parallel current density and voltages of transition layers in the Io-Jupiter system. If the ionospheric proton density decreases at the same rate as the parallel current density, the timescale on which the high-altitude transition layer disappears is consistent with the longitudinal extent of the Io tail aurora. The voltages of the high- and low-altitude transition layers remain constant until the auroral cavity disappears, as expected from observations. These results suggest that the origin of the current-voltage relationship of the Io tail aurora is the same decrease rate of the ionospheric proton density as the parallel current density.

## Relationship between the occurrence frequency of Jovian substorm-like event and plasma density in the magnetosphere

MIZUGUCHI, Takahiro<sup>1\*</sup>, MISAWA, Hiroaki<sup>1</sup>, TSUCHIYA, Fuminori<sup>1</sup>, OBARA, Takahiro<sup>1</sup>, KASAHARA, Satoshi<sup>2</sup>

<sup>1</sup>PPARC, Tohoku University, <sup>2</sup>ISAS/JAXA

Jupiter has the largest magnetosphere in the planets of solar system, which has been produced by its rapid rotation period (about 10hours), strong intrinsic magnetic field and internal source of heavy plasma originated from Io.

The observations of the Galileo orbiter revealed that there are quasi-periodic flow bursts of energetic particles and the variation of the B-theta component implying magnetic reconnections in the Jovian magnetosphere. The signatures of these events are similar to the terrestrial substorm, so they are called substorm-like events.

In the preceding studies (Kronberg et al., 2007; Woch et al., 1998), their generation processes are proposed as follow based on a hypothesis of plasma mass loading in the Jovian magnetotail region; First, the magnetotail is stretched because of the large centrifugal force by the rapid rotation and heavy ions. Second, a reconnection occurs and a plasmoid is released. Third, the magnetic field configuration returns to the initial (non-stretched) state, but then the magnetotail stretching starts again and the cycle repeats to make the periodicity.

Studying physical processes of the events is important to understand global dynamics of the Jovian magnetosphere. Their characteristics, such as their variable periodicity (2.5 - 7 days) and existence of unobserved period etc., have been known well, however, it has not been revealed yet what factor controls the periodicity of the events.

In this study, we have examined the plasma mass loading hypothesis by investigating the plasma density inside the plasma sheet by using the data obtained by the Plasma Wave Subsystems (PWS), Energetic Particle Detector (EPD) and Magnetometer (MAG) onboard the Galileo orbiter.

As a result, it is suggested that there is some correlation between electron density in the magnetotail region obtained from the plasma frequency and the occurrence frequency of the substorm-like events derived from the changing of the north-south component of the magnetic field from the preceding study by Vogt (2010), and that there is also some correlation between energetic sulfur ion density and the occurrence frequency. These results support the proposed hypothesis; the Jovian substorm-like events are driven by an internal process.

Keywords: Jupiter, Jovian magnetosphere, magnetospheric dynamics, substorm, plasma density, Galileo



## Reconsideration of generation processes of Jupiter's Io-related radio emission

MISAWA, Hiroaki<sup>1\*</sup>

<sup>1</sup>PPARC, Tohoku Univ.

The following questions; 'What kind of magneto-ionic wave Jupiter's auroral radio emission is?' and 'How the radio emission is generated?' have been long years of subjects. I have investigated the subjects based on numerical calculations using several kinds of magnetic field and plasma density models, however, the questions have not been resolved yet: a hypothesis of a special energy transporter which does not meet with the observation results was needed. Recently Jupiter's new magnetic field model 'VIPAL' was proposed based on the satellites' foot print aurora data observed by the Hubble Space Telescope (Hess et al., JGR, 2011). I have tried to make a 3D raytracing analysis for Io-DAM using the VIPAL model. The preliminary analyses show that R-X mode waves are preferable as Io-DAM and the VIPAL gives more natural explanations for the origin of Io-DAM, though there still remain some questions on restriction of 'Io-DAM' and on origin of Io-C.

Keywords: Jupiter, Io, decametric radiation, generation process, magnetic field model

## Extension of HF radio observation system in Fukui University of Technology through the introduction of GnuRadio

NAKAJO, Tomoyuki<sup>1\*</sup>, AOYAMA, Takashi<sup>1</sup>

<sup>1</sup>Department of Electrical,Electronic and Computer Engineering, Fukui University of Technology

In Fukui University of Technology, radio observations in HF band (20-40MHz) have been carried out from 2000 for Jovian decameter radiation and Solar radio bursts. At the observation site which is located at Awara campus (N36deg., E136deg.), 3 antenna towers height of 20m was set up and 9-elements cross log-periodic antenna was mounted at the top of each tower. The observation system has worked as 3 short baseline interferometer system with a baseline length of 100m class.

In Fukui University of Technology, "Formation of research centers involved in the measurement and conservation of the environment in Hokuriku region" project has been started from 2011 with the support of MEXT. In the project, we are planning to take advantage of the radio observation system in Awara campus for observation and monitoring of lightning or thunder storm activity. Therefore, we are currently developing a high-performance receiving system by introducing software-defined radio (SDR) GnuRadio+UHD into our observation system in order to realize wideband waveform observation.

GnuRadio+UHD is an open software package which consists of a lot of signal processing blocks written by C++. A user can produce one's own receiving system by combining of a user-made program using the signal processing blocks and a digital receiver. Currently, we are investigating the performance of GnuRadio+UHD with USRP2 (Universal Software-defined Radio Peripheral) supplied by Ettus Research Co. Ltd. as a digital receiver. As the result of performance test carried out so far, it has been clarified that this system has characteristics of (i) wideband (1-250MHz), (ii) high sampling rate (25MHz), (iii) wide dynamic range (90dB) and (iv) high phase stability. We conclude that this SDR system has a good performance as a receiver for interferometer system and are scheduled to advance the development of new observing system by using GnuRadio+UHD.

Keywords: software-defined radio, GnuRadio, USRP, radio observation

## Averaged characteristics of flux distributions and variations in Jovian infrared H3+ aurora: Comparison with UV's

NOGUCHI, Eriko<sup>1\*</sup>, Takeshi Sakanoi<sup>2</sup>, Yasumasa Kasaba<sup>1</sup>, Takeru Uno<sup>1</sup>, Takuya Kitami<sup>1</sup>, Chihiro Tao<sup>3</sup>, Takehiko Satoh<sup>3</sup>

<sup>1</sup>Planetary Atmosphere Physics lab.,Dept. of Geophysics, Tohoku Univ., <sup>2</sup>Planet. Plasma Atmos. Res. Cent., Tohoku Univ, <sup>3</sup>ISAS/JAXA

This study is using imaging data that Satoh et al. observed Jovian infrared H3+ aurora for long term, and it's purpose is to suggest the typical flux distribution, variation and the picture of intensity variation in each auroral region. The aurora emitted UV wavelength ray in Ly-alpha band is observed by Hubble Space Telescope (HST), and it's data is more higher space resolution and more shorter time interval. So, We consulted on analysis approach, which is taken until now, to enable to compare characteristic between IR aurora and UV aurora.

Jovian Auroral flux distribution and the variation is different by mapping magnetospheric region. Auroral high latitude region, mapping open flux, shows variation driven by Solar wind at short times. On the other hand, Main oval, mapping inner magnetospheric region, is considered that more stably exists, because the energy source, that high Jovian rotation ingenerates, effects brightening. There is a direct temporal-spatial correlation between UV aurora and injected electron, because H and H2 directly emit electric transition emission.

On the other hand, The IR auroral process is that H2 and H2+ ,injected particle produced, collided with each other, and this event produced H3+ and thermal excitation of H3+ emit infrared ray. So, IR aurora reflects thermospheric temperature and may be different from the picture of UV auroral flux distribution and intensity variation.

In Nichols et al.,2009, They first resulted in Jovian UV auroral typical flux distribution ,using data Hubble Space Telescope observed emitted UV wavelength ray for two months. This analysis circularly separated auroral region, and shows the response of solar wind dynamic pressure and correlation between each auroral region.

In this study, we apply UV auroral flux distribution in Nichols et al.,2009 to IR auroral region with the intent to verify difference of the characteristic UV aurora showed.

About analysis data, we use image data observed emitted infrared ray by NSFCAM using 3.4265um narrow bandpass filter attached to NASA/IRTF in 1995-2004, and The typical seeing of this data is 1arcsec(under 0.1 arcsec in HST data). Observational days are discrete, however, we can analyze 57days worth of data. Thus far, we compare between dynamic pressure and the intensity variation during dynamic pressure is continually high or low for several days. About the dynamic pressure, we refer to 1DMHD model extrapolates solar wind observed near earth to Jovian orbital.

(A) There is slightly not only the positive correlation between in high latitude region and dynamic pressure, but also it in main-oval region and dynamic pressure( $r=0.8$ ). (B) While there is the positive correlation between the variation of intensity in high latitude region and in main-oval region is high similar to UV's, the polar inner region is more brighter than UV's. The latter is seen in Saturn, it is considered that upper high latitude region is more heat reflected the adiabatic compression.

In main oval region, the typical emitted power is 334.1GW , and the range of variation is 180.86GW-613.01GW.

After this, we will progress to analyze data all over. There is potentially four problems, but they are fatally common problems in past Jovian auroral observation.

(1) The spatial resolution is one digit lower than HST data, (2) This analysis data isn't simultaneous observation between the IRTF observation and the HST observation, (3) There is the period of low accuracy of solar wind (5 days), (4) The number of data isn't enough to bung up compared to response time of Jovian magnetosphere.

In this presentation, based on above-reference, we will report tentative result using all data.

## Development of the InSb array sensor drive system for infrared observations

KITAMI, Takuya<sup>1</sup>, SAKANOI, Takeshi<sup>1\*</sup>, KASABA, Yasumasa<sup>1</sup>

<sup>1</sup>Dep. Geophysics Graduate School of Science Tohoku University

Jupiter is a biggest planet in the solar system. There are the aurora phenomena in UV, Visible and IR range that reflected magnetosphere activity. Especially, in  $H_2$   $H_3^+$  NIR aurora, ground based observation is possible because earth atmosphere transmissivity is high. So  $H_2$   $H_3^+$  aurora are suitable for long-term observation.

However, the number of the devices is limited by difficulty of the development of the infrared measurement, and it is difficult to observe long-term continuation from a problem to large-sized telescope machine time. The development of the infrared imaging camera is carried out in Takahashi (2005) so far in Tohoku University, and the development of the infrared echelle spectrum device is carried out in Uno (2009).

However, the problem that a count level of the output image did not change into even if I changed an exposure occurred because it was defective in infrared sensor (InSb sensor) drive system. Radical new development InSb sensor drive used for these devices was started in the Kobuna (2008). It is the joint development with the Tohoku University astronomy specialty Professor Takashi Ichikawa classroom, and the design of the analog circuit is performed in an astronomy classroom, and this development examined digital circuit pro-development and synthesis movement in Kobuna (2008),but does not reach the completion.

It is expected what is utilized as drive system of the infrared imaging device which I produced in Takahashi (2005) and the infrared echelle spectroscope that development was carried out in Uno (2009). The InSb sensor drive system can contribute to continuation observation for a long term of the planetary atmosphere including Jovian IR aurora.

## Development of a New Telescope Dedicated to Observation of Planets at Haleakala, Hawaii : VIII

OKANO, Shoichi<sup>1\*</sup>, KAGITANI, Masato<sup>2</sup>, KASABA, Yasumasa<sup>2</sup>, SAKANNOI, Takeshi<sup>2</sup>, OBARA, Takahiro<sup>2</sup>, Isabelle Scholl<sup>3</sup>, Jeffrey Kuhn<sup>3</sup>

<sup>1</sup>Dep. Geophysics, Tohoku Univ., <sup>2</sup>PPARC, Tohoku Univ., <sup>3</sup>IfA, Univ. Hawaii

We are constructing a 1.8m new telescope at the summit of Mt. Haleakala, Maui, Hawaii. It is under the collaboration with the Institute for Astronomy (IfA), University of Hawaii. In 2011, the fabrication of the primary mirror has been done. And plans of development timeline, facilities required for the development, telescope mechanical structure, and the dome were made. In 2012, we will start actual development along the timeline, and go into the most key phase in the development. The first light will be, if everything goes well, in 2014.

Clear sky and good seeing condition are definitely important for any ground-based observations. The summit of Mt. Haleakala in Maui, Hawaii is not the highest place (elv. 3050m), but one of the best sites with clear skies, good seeing, low humidity conditions, and good accessibility for us. At the Haleakala High Altitude Observatory at the summit, our group has been operating a 40cm Schmidt-Cassegrain telescope, and we have so far observed faint atmospheric and plasma features around bright planets, Io plasma torus, Mercury and Lunar sodium tail, and so on. Atmospheric escapes from Mars and Venus, the exoplanets close to mother stars are also possible topics. However, when we try to observe those faint emissions surrounding the bright objects, intense scattered light is always the most serious problem.

The new project, called PLANETS (Polarized Light from Atmospheres of Nearby Extra Terrestrial Planets), is dedicated to the observation of solar system planets and exoplanets. It consists of an off-axis primary mirror with a diameter of 1.8m, and Gregorian optics on an equatorial mount. State-of-the-art adaptive optics and masking technologies will be adopted to eliminate the scattering light. Based on these designs, it can avoid diffractions due to a spider structure that holds a secondary mirror and to minimize the scattered light from mirror surfaces as far as possible. In addition, the telescope optics will have a ultra-smooth mirror surface, the roughness of less than  $1/20$  lambda, with a new polish technology called HyDra, a water jet polishing technology developed by a group at Univ. Nac. Aut. de Mexico (UNAM). (This project is also a test for this new technology applied to off-axis mirrors.) Since a telescope completely optimized to a wide dynamic range does not exist yet, it can provide us a unique facility for spectroscopic and polarimetric observations of faint environments around the bright bodies, like planetary environments, stellar disks, etc.

This project is based on the collaboration among PPARC / Tohoku Univ., IfA / Univ. Hawaii (USA), Kiepenheuer Inst. Sonnenphysik (Germany), UNAM (Mexico), Univ. Turku (Finland), Harlingen Center for Innovative Optics (Canada), Stan Truitt (USA), Craig Breckenridge (Canada), and other collaborators. In 2011 March, after the Earthquake, the primary mirror glass blank completed in Japan was shipped to US, and now in the generating process. We also established the team structure, development timeline, and facilities required for the development. The main development will be at ATRC (Advanced Technology Research Center) of IfA in Maui. In 2012, all designs of the telescope mechanical structure and the domes will be finalized, and construction of development facility and structures will actually be started.

For promoting the project, Dr. Kagitani has been staying in Maui in 2011FY, and is contributing to the optical fiber Echelle spectrograph developments at ATRC. From June 2012, Prof. Okano will also be staying at ATRC/IfA. Associated with such residence, we are also preparing to move a 60cm telescope of Tohoku Univ. to the summit. In the paper, we summarize the overview of our drastic steps toward this future expected in this year.

Keywords: PLANETS, telescope project, optical and infrared, planetary observations